

## DEFORMATION TEXTURES IN PYRITE FROM THE VANGORDA Pb-Zn-Ag DEPOSIT, YUKON, CANADA

### Abstract

The Vangorda Pb-Zn-Ag orebody is a 7.1 M tonne, polydeformed strataform massive sulphide deposit in the Anvil mining district, Yukon, Canada. Five sulphide lithofacies have been identified within the deposit with a typical mineralogy of pyrite, sphalerite, galena, and barite. Pyrrhotite-sphalerite-magnetite assemblages are locally developed. Etched polished sections of massive pyrite ores display relict primary depositional pyrite textures such as colloform growth zoning and spheroidal/framboidal features. A wide variety of brittle deformation, ductile deformation, and annealing textures have been identified. Brittle deformation textures include thin zones of intense cataclasis, grain indentation and axial cracking, and grain boundary sliding features. Ductile deformation textures include strong preferred grain shape orientations, dislocation textures, grain boundary migration, dynamic recrystallisation and pressure solution textures. Post deformational annealing has produced grain growth with lobate grain boundaries, 120° triple junctions and idioblastic pyrite porphyroblasts.

The distribution of deformation textures within the Vangorda orebody suggests strong strain partitioning along fold limbs and fault/shear zones. It is postulated that focussed fluid flow in these zones had significant effects on the deformation of these pyritic ores.

## Introduction

The Vangorda deposit is a 7.1 million tonne (Jennings and Jilson, 1986), SEDEX-type (Carne and Cathro, 1982) massive sulphide orebody in the Anvil Pb-Zn-Ag District, Yukon Territory, Canada (fig. 1). The deposit has a combined Pb + Zn grade of 7.7%. It has been polydeformed and polymetamorphosed under mid-greenschist facies conditions (Tempelman-Kluit, 1972; Jennings and Jilson, 1986). The Vangorda orebody is a shallowly southwesterly dipping, with complex and folded lenses of massive and disseminated sulphides and barite approximately 900 m long, 100 m wide and varying in thickness from 20 to 60 m. The orebody is currently being mined in a 10,000 tonne per day open pit operation by Curragh Resources. The deposit consists of highly folded lenses of pyrite-sphalerite-galena and barite in quartz muscovite phyllites and ribbon banded quartzites. Five distinct sulphide lithofacies with varying modal abundances of pyrite have been identified. Pyrite within these display a variety of brittle and ductile deformation features, together with recrystallisation, and annealing textures (Brown and McClay, 1992).

Pyrite in many deformed and metamorphosed ore-bodies, as well as in controlled experiments, has been shown to deform by brittle mechanisms over a wide range of geological conditions (e.g. Vokes, 1969, 1971; Ramdohr, 1969; Graf and Skinner, 1970; Atkinson, 1975; Mookherjee, 1976; McClay, 1983). It has further been demonstrated that both experimentally and naturally deformed pyrite also deforms by crystal plastic mechanisms, and diffusive mass transfer coupled with grain boundary sliding (Mookherjee, 1971; Natale, 1971; Couderc et al., 1980; Graf et al., 1981; Cox et al. 1981; McClay and Ellis, 1983; Brill, 1989). Cox et al. (1981) experimentally determined the onset of crystal plastic mechanisms in pyrite to occur at approximately 450°C at 300 MPa. Dynamic recrystallisation, though not a widely reported feature in naturally deformed pyrites, has also been found to occur (e.g. Cox et al.,

1981). This paper examines deformation and annealing textures in pyrite from the Vangorda deposit. Data for this study comes from logged diamond drill holes and from detailed mapping and sampling of the open pit.

## Regional Geology

The Anvil lead-zinc-silver district is located within the Omineca Crystalline Belt of the northern Canadian Cordillera, approximately 200 km northeast of Whitehorse, Yukon (fig. 1). Rocks in the Anvil District consist of a structurally thickened sequence of late Precambrian to upper Palaeozoic polydeformed, polymetamorphosed, metasedimentary and metavolcanic schists and phyllites (Jennings and Jilson, 1986). These have been intruded by Cretaceous granites and granodiorites (Pigage and Anderson, 1985). The Anvil District is host to five major stratiform, massive sulphide deposits that lie along a northwest-southeast curvilinear trend, parallel to the regional structural grain of the district (fig. 2).

### Lithostratigraphy

The lithostratigraphy of the Anvil District is shown in fig. 3. Precise thickness and age determinations are difficult because of the penetrative deformation and metamorphism. Within the Anvil District two lithostratigraphic units, the lower non-calcareous Mt. Mye Formation phyllites and the overlying calcareous Vangorda Formation phyllites are regionally significant as the sulphide deposits straddle the boundary between them (fig. 3). The Vangorda orebody occurs in the Mount Mye Formation immediately below the base of the Vangorda Formation. In the vicinity of the Vangorda deposit the Mt. Mye and Vangorda formations are typically mid-greenschist facies chlorite-muscovite phyllites.

### Deformation events

Five deformation events have been recognised in the Anvil District, the first two of which ( $D_1$  and  $D_2$ ) are regionally significant (Jennings and Jilson, 1986).  $D_1$  is interpreted to be related to northeast-directed folding, thrusting, and nappe emplacement during the pre- to mid-Cretaceous docking of allochthonous terranes from the southwest onto the ancestral margin of North America (Gabrielse and Yorath, 1989).  $D_1$  deformation resulted in the development of NE-verging  $F_1$  folds and a penetrative regional foliation ( $S_1$ ), and regional metamorphism. The  $D_2$  tectonic setting appears to be similar to that of a metamorphic core complex and is related to emplacement, uplift, and unroofing of the Anvil Batholith.  $D_2$  resulted in southwest-directed folding, development of a shallowly SW-dipping, penetrative foliation ( $S_2$ ), and greenschist to amphibolite facies metamorphism (Jennings and Jilson, 1986; Smith and Erdmer, 1990). Brittle to ductile extensional faulting, related to unroofing of the Anvil Batholith, is late- to post- $D_2$  folding (Pigage and Jilson, 1985).  $D_3$  to  $D_5$  deformation events produced minor folding and steeply dipping crenulation foliations that variably overprint the  $D_1$  and  $D_2$  structural elements.

### **The Vangorda Deposit**

The Vangorda deposit occurs 50 to 120 meters beneath the base of the Vangorda Formation (fig. 3). The orebody plunges shallowly towards the northwest and is interpreted to occur in the hinge and the under limb of an overturned large-scale  $F_2$  fold (fig. 4) (Jennings and Jilson, 1986; Pigage, 1990). Syn- to post  $D_2$  NW - SE oriented extensional faults truncate the deposit to the northwest and southeast (Pigage, 1990; Brown and McClay, 1992).

### Ore Lithofacies

The Vangorda orebody consists of a number of sulphide lenses of varying

thickness (1 - 30m) and varying sulphide composition that are typically accompanied by a footwall biased phyllitic, muscovite-chlorite alteration zone. In any one section or drill hole the entire ore sequence as shown in fig. 3 may or may not be developed. The salient features of each ore lithofacies in the Vangorda deposit are outlined below.

Ribboned-banded, carbonaceous, pyritic quartzite: This is a well banded, sulphide-bearing quartzite, with minor sphalerite and galena. Bands are on a millimetre- to centimetre-scale and consist of quartz-sulphides and carbonaceous quartzite. Pyrite grain size ranges from 0.1 mm to 1.0 mm.

Pyritic quartzite: This consists predominantly of quartz with up to 40% pyrite and minor sphalerite and galena. These rocks have a moderate to poorly developed pyrite banding with, locally, a well developed micaceous (muscovite) foliation. Pyrite typically forms 0.1mm - 1mm sized subhedral to euhedral porphyroblasts, with local coarse grained patches in which grain size reaches approximately 3.0 mm. Galena, and less commonly sphalerite, occur in coarse-grained patches with grain sizes ranging from 0.05 to 0.5mm.

Massive pyritic sulphides: These are typically massive pyrite with minor sphalerite, galena, pyrrhotite, and magnetite. Quartz, barite, and carbonates are disseminated throughout or occur in coarse aggregates. Total pyrite content varies from between 60% to close to 100% with grain size ranging from 0.1 to 1.5mm.

Baritic, massive pyritic sulphides: These consist predominantly of barite with pyrite, sphalerite, galena, with minor magnetite. Quartz and carbonate are major matrix components. Clasts of massive pyrite and phyllite are common. Total barite content varies but may be as high as 50%.

As well as the above lithofacies, the distribution of which is interpreted to

reflect primary depositional ore types, another lithofacies occurs in areas of high strain and is interpreted to be the result of metamorphic reactions and strain related mobilisation during deformation.

Pyrrhotite-sphalerite-pyrite-galena (breccia): This lithofacies is a variant of the pyritic quartzite in which the dominant sulphides are pyrrhotite and sphalerite with lesser pyrite, and galena. Coarse patches of sphalerite or galena are common. Pyrite typically occurs as 0.1 to 1.5mm-sized porphyroblasts and as isolated breccia clasts. This lithofacies is typically highly strained and often contain clasts of other rock types and a well developed anastomosing foliation. Tailed clasts and rolling structures are common.

#### Deformation of the Vangorda deposit

All rocks in the Vangorda deposit have been penetratively deformed and metamorphosed by  $D_1$  and  $D_2$  deformation events, making definition of any primary depositional features on a scale other than microscopic (see below) ambiguous at best. Direct evidence of  $F_1$  folding is restricted to refolded folds in drill core and in pit wall exposures, suggesting that  $F_1$  folding may have played an important role in the present geometry of the deposit. In most of the ore lithofacies a  $S_1$  pyritic banding is well developed on a scale of millimetres to centimetres. In the phyllites and in the ribbon banded, carbonaceous quartzite,  $S_1$  is commonly preserved as lithons in the hinges of  $F_2$  folds. In the more sulphide-rich lithofacies, however,  $S_1$  is typically transposed into subparallel to the  $F_2$  axial surfaces.

The dominant fold phase in the Vangorda deposit is  $F_2$ .  $F_2$  folds are shallowly east-west to northwest-southeast-plunging, tight to near-isoclinal (interlimb angle is commonly between  $5^\circ$  to  $25^\circ$ ) similar style folds.  $F_2$  fold morphology varies according to lithofacies as a result of different rheologies, but in general a similar style is maintained.

In the surrounding phyllites, a penetrative sub-horizontal, wavy  $F_2$  axial surface foliation ( $S_2$ ) is developed. In some sulphide lithofacies, such as the ribboned-banded, carbonaceous quartzite, a differentiated axial planar  $S_2$  foliation is also well developed. However,  $S_2$  appears to be non-penetrative in the sulphides and is only found rarely in fold hinges. In high strain zones,  $S_1$  banding in the sulphide lithofacies is discontinuous as a result of shearing and a new, inhomogeneous  $S_2$  foliation is developed. In ore rocks with a  $S_2$  foliation (such as the ribbon-banded, carbonaceous quartzite) pyrite porphyroblast often grow across the foliation indicating post- $S_2$  pyrite growth.

Thin, discontinuous, anastomosing shear zones are widespread in the deposit, and are typically parallel to the  $S_2$  orientation (figs 4 & 5). Within these zones, massive pyrite has deformed by brecciation whereas other sulphides, such as pyrrhotite, sphalerite, and galena, have deformed by ductile mechanisms.

The Vangorda deposit is very strongly faulted by steeply northwest- to southeast-dipping brittle extensional faults that, together with  $F_2$  folding, provide the dominant structural control on the present geometry of the orebody. All extensional faults examined truncate the  $S_2$  foliation and  $F_2$  folds and therefore clearly post-date or are late  $D_2$  (Brown and McClay, 1992). Faults have an apparent offset of centimetres to (tens) metres but, due to paucity of marker horizons, it is often impossible to determine the exact amount of offset on any one fault. Pyrite slickensides on polished fault surfaces typically have a shallow pitch angle suggesting a late stage strike-slip to oblique-slip phase of fault movement.

A number of low-angle, post- $D_2$ , northeast-directed thrusts occur within phyllites in the southeast end of the deposit. These thrusts cut the  $S_2$  foliation, and locally the extensional faults, and have offsets ranging from centimetres up to several tens of metres.

## Microstructures

Representative samples were taken from each lithofacies to determine the deformation mechanisms and metamorphic reactions active on a mesoscopic and microscopic scale and their relationship to structural position. For the purpose of this study, selected pyrite polished sections were etched with warm 20%  $\text{HNO}_3$  to study growth features (e.g. grain boundaries and overgrowths), different mineral phases, and deformation textures (e.g. dislocation, diffusion and recrystallisation structures).

Tempelman-Kluit (1970) and McClay and Ellis (1983) noted a crude correlation between pyrite grain-size and metamorphic grade in the Anvil District deposits. McClay and Ellis (1983) also noted a number of other factors that affect grain-size including primary/depositional and post-depositional/metamorphic effects as well as the nature of the matrix, the nature of grain boundaries, and pyrite chemistry. In the Vangorda orebody pyrite porphyroblasts exhibit both brittle and ductile deformation textures as well as post deformation annealing features, all of which affect grain-size to varying degrees. Sulphide grain-sizes and textures are significant metallurgical factors affecting the milling properties of massive sulphide ores. Rigorous textural analysis using etched sections is of fundamental importance for understanding the depositional through metamorphic evolution of the deposit.

Pyrite grain-size in the Vangorda deposit ranges from 0.1mm to 1.5mm, with an average grain-size of between 0.5 mm and 1.0 mm. Large grains (i.e. in the 0.5 mm to 1.0 mm range) are typically equant to idioblastic metamorphic porphyroblasts. However, relict, primary colloform pyrite grains and relict spheroids and framboids, although rare, can still be found. The colloform and zoned grains are typically 0.1mm to 0.25mm sized, equant to xenoblastic and occur alone or, more commonly, as cores

in metamorphic porphyroblasts (fig. 6a).

### Brittle deformation textures

Deformation of single grains and massive pyrite in the Vangorda deposit occurred mainly by cataclasis, with the result of an overall reduction in grain-size. Cataclastic textures, in the form of brittle shear zones in massive pyrite and fracturing and grain boundary sliding are found throughout the deposit, regardless of structural position. Zones of intense brittle shearing are common in polycrystalline pyrite and form aggregates of finely crushed, angular grains (fig. 6b). These zones are commonly sealed by quartz, carbonate, and mica. In places, smaller fractures, oriented approximately 30° to the shear zone boundary, cross-cut the shear zone and may be interpreted as Riedel fractures.

On a grain scale, where pyrite grains impinge upon each other, indentation and dissolution, axial cracking and microfracturing occur (fig. 6c). Locally, pyrite displays internal microfracturing, suggesting inelastic strain accommodation in the core of the grains. Grain boundary sliding, which is geometrically necessary to accommodate diffusional deformation, is usually difficult to document. Microfracturing along and parallel to grain boundaries where two grains impinge upon each other indicates that grain boundary sliding was active (Fig. 6d).

### Ductile deformation features

Readily identifiable ductile deformation textures in pyrite in the Vangorda deposit are not widespread but are found locally, commonly in zones of high bulk strain such as the overturned limbs of folds. The lack of ductile deformation features is most likely a result of post deformation, strong annealing, that produced grain growth and an increase in grain-size.

Dislocation microstructures in pyrite are characterised by straight to slightly curved, stepped, or branching dislocation etch pits that outline dislocation tangles and walls forming parallel to  $\langle 100 \rangle$  and  $\langle 110 \rangle$  (cf. Cox et al., 1981; Graf et al., 1981). Movement of dislocations through the crystal, possibly along the  $\{100\} \langle 001 \rangle$  slip plane, is evidenced by slip lines (fig. 7a), here bent to form kink bands. Etch pits commonly intersect to form grid-like arrays that mark subgrain boundaries and the onset of polygonisation (fig. 7b). The subgrains are 1  $\mu\text{m}$  to 10  $\mu\text{m}$  in size.

Dynamically recrystallised grains are common in the samples looked at in this study. Subgrain formation commonly occurs along the boundaries of parent grains (fig. 7c) and in extreme cases result in the formation of a core mantle texture. Recrystallised grains are typically 5  $\mu\text{m}$  - 50  $\mu\text{m}$ , equant grains with straight to slightly curved grain boundaries. Post-recrystallisation grain growth has likely resulted in an increase in grain-size from the smaller subgrains.

Preferred grain shape orientation in pyrite (fig. 7d) occurs in areas of high bulk strain in which thin, discontinuous, often anastomosing zones define a crude  $S_2$  foliation. Grains are elongate with straight to slightly curved, mildly sutured, and lightly indented grain boundaries. Within individual grains there is little or no evidence of brittle deformation, and dislocation textures are rare. These features are particularly well displayed in aggregates of small grains which have relict spheroidal and framboidal cores (fig. 7e). In addition, overgrowths are not apparent on elongate grains, but pyrite porphyroblasts elsewhere in these samples commonly do have overgrowths. Fluid assisted diffusive mass transfer - 'pressure solution' is thought to be the likely mechanism responsible for formation of this preferred grain shape fabric (cf. McClay and Ellis, 1984). These features suggest dissolution and mobilisation have occurred, at least on a grain scale.

### Annealing textures

As well as deformation textures, pyrite shows a number of annealing and grain growth textures due to metamorphism. In the massive pyritic lithofacies, grains are commonly 0.2mm to 1.5mm in size, equant with straight to mildly sutured grain boundaries that meet at  $120^{\circ}$  triple junctions (fig. 7f). Strongly lobate grain boundaries are indicative of grain growth during annealing. Other sulphide phases, as well as quartz and carbonate, are commonly trapped along grain boundaries and at triple junctions. Concentric inclusion patterns in pyrite grains suggest multiple phases of grain growth. Rare, helicitic inclusion patterns indicate either porphyroblast rotation or multistage porphyroblast growth overgrowing successive foliations (cf. Bell, 1985).

## **Discussion**

The Vangorda orebody has undergone polyphase deformation and metamorphism under greenschist facies conditions. Five distinct sulphide lithofacies have been recognised (Brown and McClay, 1992) and their textures reflect the response of the sulphides to various degrees of brittle and ductile deformation.

Primary depositional pyrite textures such as colloform and growth banded grains together with relict spheroidal and framboidal aggregates are only rarely preserved in the Vangorda sulphides. Deformation, recrystallisation and grain growth textures predominate. Pyrite deformation textures identified in this study include brecciation in cataclastic shear zones, grain fracturing, grain boundary sliding, preferred pyrite grain shape orientations, pressure solution, dislocation structures (slip lines and dislocation walls), subgrain formation and

dynamic recrystallization indicate that the pyrite in the Vangorda deposit deformed by both brittle and ductile mechanisms. These deformation processes, in general, have led to an overall reduction in grain-size. Post deformation annealing has resulted in an increase in relative grain-size, formation of equant grains and development of pyrite porphyroblasts.

Grain fragmentation and axial cracking indicate that brittle deformation of pyrite grains and of the massive pyrite has occurred throughout the deposit. Breccia textures and pyrrhotite-magnetite sphalerite shear zones are localised in high strain zones (fig. 5) that appear to be anastomosing  $D_2$  fault zones on the limbs of the  $D_2$  fold (fig. 4). Similarly textures indicating strong plastic deformation of pyrite (bands of dynamically recrystallised grains and preferred grain-shape textures) are also restricted to localised areas. The partitioning of deformation textures, both brittle and ductile, within the Vangorda orebody may be interpreted to indicate local strain or strain-rate partitioning during deformation. As the orebody and host rocks appear to be uniformly metamorphosed at mid greenschist facies conditions, the brittle and ductile strain partitioning indicates local variations in sulphide/matrix rheologies. High strain zones may be localised on the limbs of  $D_2$  folds or along  $D_2$  fault zones. Reaction enhanced ductility may have been produced by the formation of pyrrhotite-sphalerite-magnetite assemblages in shear zones.  $D_2$  fault zones may also have been the locus of transient high porefluid pressures that permitted the deformation to occur well into the cataclastic deformation regime thus producing the breccia textured pyrites.

The plastic deformation textures in pyrite found in this study (slip lines, kink bands, subgrains, dynamically recrystallised grains and preferred grain shape orientations) also indicate that, at geological strain rates, plastic deformation of pyrite occurs well below the threshold of  $450^\circ\text{C}$  at 300 MPa confining pressure determined experimentally in the laboratory (Cox et al., 1981). In addition relict deformed spheroidal and framboidal textures (fig. 7e) together with overgrowth features indicate

that pressure solution played an important role in the deformation of pyrite in the Vangorda deposit.

Post deformational thermal annealing in the Vangorda deposit, as in the other Anvil District deposits (e.g. Faro - McClay and Ellis, 1983), resulted in the formation of foam textures with  $120^\circ$  triple junctions together with grain boundary migration, grain growth and porphyroblast formation. The annealing event has largely obscured and destroyed the earlier depositional, diagenetic, overgrowth and deformation textures tending to increase the grain size and produce homogeneous granoblastic pyrite ores.

The tight to isoclinal, similar fold style and complex internal deformation indicates that the Vangorda deposit has undergone significantly high strains. Strain partitioning has produced breccia zones and shear zones in part controlled by the sulphide and matrix rheologies. Shear zones in particular are localised in the baritic massive sulphide facies. Shear zones have long been known to act as conduits for fluids during deformation (e.g. Carter et al., 1990, and references therein), and fluids are well known to effect the mechanical response of rocks during deformation (e.g. Hubbert and Rubey, 1959; Handin et al., 1963; Atkinson, 1984). To date, a full appreciation of the role of a fluid in the deforming Vangorda deposit has not been assessed. However, sealing of cataclastic zones and fractures by quartz, carbonate, and often pyrite, together with the occurrence of overgrowths on grains indicates that fluid infiltration and mobilisation did occur, and likely played an important role in the mechanical response of the sulphide rocks.

The precise effects of pore fluids on the ductile deformation of pyrite is largely unknown, and is beyond the scope of this paper. Textural evidence, however, indicates that pressure solution is an important deformation mechanism in naturally deformed pyrite (McClay and Ellis, 1983; McClay, 1991). It may be expected that the focussing of a fluid

phase along zones of increased strain (i.e. shear zones) may significantly reduce the flow stress required to induce crystal plastic deformation in pyrite, in much the same way it affects the mechanical response of quartz and olivine (Blacic, 1972; Kirby, 1984; Kirby and Kronenberg, 1987). The effects of fluid chemistry on rock and mineral deformation are not well understood, although Hobbs (1981, 1984) suggests that deformation and metamorphic reactions are closely tied. The deformation of pyrite in deposits such as Vangorda may be expected to have not only dramatically changed the textural characteristics of the ore but may also be expected to have affected the chemical and isotopic signatures.

## Acknowledgements

This study forms part of D.Brown's Ph.D. research program. Brown is funded in part by the Rothemere Foundation and by the Special Scholarship for Students doing Research in Resource Development administered by Memorial University of Newfoundland. Fieldwork was supported in part by Curragh Resources, Department of Indian and Northern Affairs, Whitehorse, Geological Survey of Canada, Vancouver, and by the Industry Association, R.H.B.N.C., University of London.

## References

- Atkinson, B.K. (1975) *Econ. Geol.* 70, 473-87.
- Atkinson, B.K. (1984) *J. Geophysical. Res.* 89, 4077-4114.
- Bell, T.H. (1985) *J. Metamorphic Geol.* 3, 109-18.
- Blacic, J.D. (1972) *Amer. Geophysical Union Mono.* 16, 109-15.
- Brill, B.A. (1989) *J. Struct. Geol.* 11, 591-601.
- Brown, D. and McClay, K.R. (1992) In Current Research, Part A. *Geol. Sur. of Canada, Paper 92-1A*
- Carne, R.C., and Cathro, R.J. (1982) *Canadian Institute Mining and Metallurgy Bull.*, Vol. 75, no.840, 66-78.
- Carter, N.L., Kronenberg, A.K., Ross, J.V., and Wiltschko, D.V. (1990) In Deformation Mechanisms, Rheology and Tectonics (R.J. Knipe and E.H.

Rutter eds.). Geol. Soc. Special Pub. 54, 1-13.

Couderc, J.-J., Bras, J., Fagot, M., and Levade, C. (1980) Bull. Mineral. 103, 547-57.

Cox, S.F., Etheridge, M.A., and Hobbs, B.E. (1981) Econ. Geol. 76, 2105-18.

Gabrielse and Yorath (1989) Geoscience Canada 16, 67 - 83.

Graf, J.L., and Skinner, B.J. (1970) Econ. Geol. 65, 206-15

Graf, J.L., Bras, J., Fagot, M., Levade, C., and Couderc, J.-J. (1981) Econ. Geol. 76, 738-44.

Handin, J., Hager, R.V., Jr., Friedman, M., and Feather, J.N. (1963) A.A.P.G. Bull. 46, 717-55.

Hobbs, B.E. (1981) Tectonophysics, 78, 335-83.

Hobbs, B.E. (1984) J. Geophysical Res., 89, 4026-38.

Hubbert, M.K., and Rubey, W.W. (1959) Geol. Soc. Amer. Bull., 70, 115-66.

Jennings, D.S., and Jilson, G.A. (1986) In Mineral Deposits of Northern Cordillera (J.A. Morin, ed.) Canadian Institute Mining and Metallurgy, Special Paper 37, 319-61.

Kirby, S.H. (1984) J. Geophysical Res. 89, 3991-95.

Kirby, S.H., and Kronenberg, A.K. (1987) Reviews in Geophysics. 25, 1219-44.

McClay, K.R. (1983) In Sediment-hosted Stratiform Lead-Zinc Deposits. Short Course Notes. Mineral. Assoc. Can. 283-307.

McClay, K.R. (1991) Ore Geology Reviews 6, 435 - 462.

McClay, K.R., and Ellis, P.G. (1983) Mineral. Mag., 47, 527-38

McClay, K.R., and Ellis, P.G. (1984) Econ. Geol. 79, 400-403.

Mookherjee, A. (1971) Econ. Geol. 66, 200.

Mookherjee, A. (1976) In Handbook of Stratabound and Strataform Ore Deposits (K.H. Wolf ed.) Elsevier, Amsterdam. 4, 203-60.

Natale, P. (1971). Rend. Soc. Italian Miner. Petrol. 27, 539-50.

Pigage, L.C. (1990) In Mineral Deposits of the Northern Canadian Cordillera, Yukon-northeastern British Columbia (J.G. Abbott and R.J.W. Turner, eds.) Geol. Sur. Canada, Open File 2169, 283-308.

Pigage, L.C. and Anderson, R.G. (1985) Can. J. Earth Sci. 22, 1204-16.

Pigage, L.C., and Jilson, G.A. (1985) G.S.A., Abstracts with Programs - Cordilleran Section, 17, 400.

Ramdohr, P. (1969) The Ore Minerals and Their Intergrowths. Pergamon Press, Oxford. 1174 pp.

Ramsay, J.G. (1967) Folding and Fracturing of Rocks. McGraw-Hill, New York, 568 pp.

Smith, J.M., and Erdmer, P. (1985) Can. J. Earth Sci. 27, 344-56.

Tempelman-Kluit, D.J. (1970) *Can. J. Earth Sci.* 7, 1339-45.

Tempelman-Kluit, D.J. (1972) *Geol. Sur. Canada, Bull.* 208. 73 p.

Vokes, F.M. (1969) *Earth-Sci. Rev.*, 95, 403-406.

Vokes, F.M. (1971) *Mineral. Deposita*, 6, 122-129.

Department of Geology, Royal Holloway      **D. Brown and K.R. McClay**  
and Bedford New College,  
University of London,  
Egham, Surrey, TW20 OEX, U.K.

## FIGURE CAPTIONS

- FIGURE 1. Location of the Anvil District in the Northern Canadian Cordillera (after Brown and McClay, 1992).
- FIGURE 2. Regional geology of the Anvil District showing the location of the Vangorda deposit (after Brown and McClay, 1992)
- FIGURE 3. Lithostratigraphy of the Anvil District (after Brown and McClay, 1992)
- FIGURE 4. Cross-section 6E, Vangorda deposit showing the tight to near isoclinal, similar fold, and the distribution of the ore lithofacies.
- FIGURE 5. Detailed logs through the sulphide stratigraphy, section 6E, Vangorda deposit.
- FIGURE 6. Pyrite textures in the Vangorda deposit. All photomicrographs are of polished sections etched with  $\text{HNO}_3$ .
- a). Relict primary colloform texture in the cores of metamorphic porphyroblasts. Nomarski interference contrast, section 90-52, DDH 90V-115.
  - b). Pyrite cataclasite in a shear zone. Note the comminution of pyrite grains and the disaggregation of clusters of pyrite grains. Nomarski interference contrast, section 90-46, DDH 90V-116.
  - c). Indentation and axial cracking of subhedral pyrite porphyroblasts. Plane polarised light, section 90-37, DDH 90V-67.
  - d). Microfracturing sub-parallel to grain boundaries indicating grain boundary sliding during deformation. Nomarski interference contrast, section 90-121, DDH 79V-95.
- FIGURE 7. Pyrite textures in the Vangorda deposit. All photomicrographs are of polished sections etched with  $\text{HNO}_3$ .
- a). Etched pyrite porphyroblast showing kink bands that bend slip lines. Straight lines of etch pits that traverse whole grains or several grains are surface scratches on the specimen. Nomarski interference contrast, section 90-41, DDH 90V-67.
  - b). Arrays of etch pits that form subgrain walls indicating the

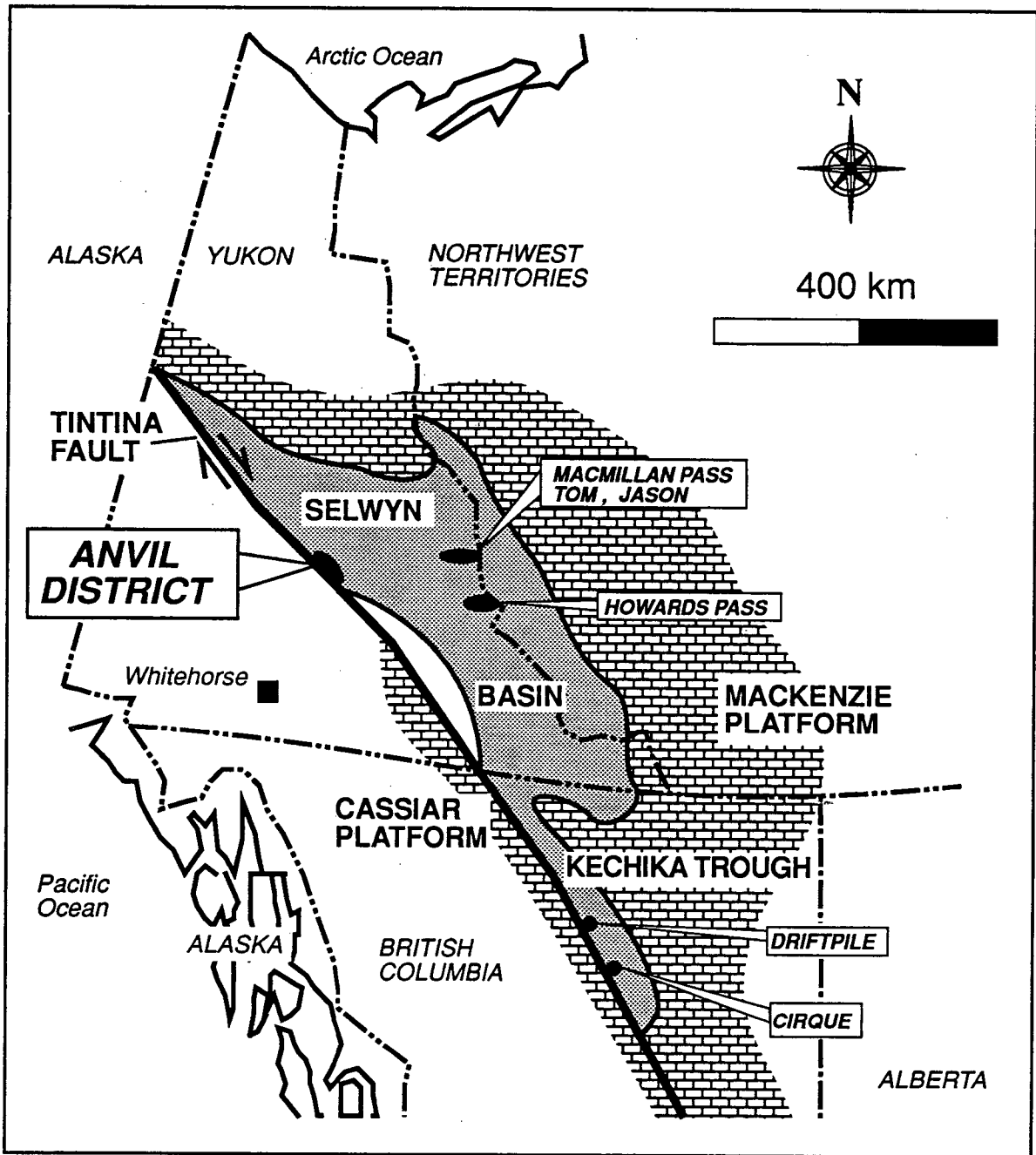
onset of polygonisation. Plane polarised light, section 90-39, DDH 90V-67.

c). Dynamically recrystallised grains formed at the margin of large old grains. Plane polarised light, Section 90-46, DDH 90V-116.

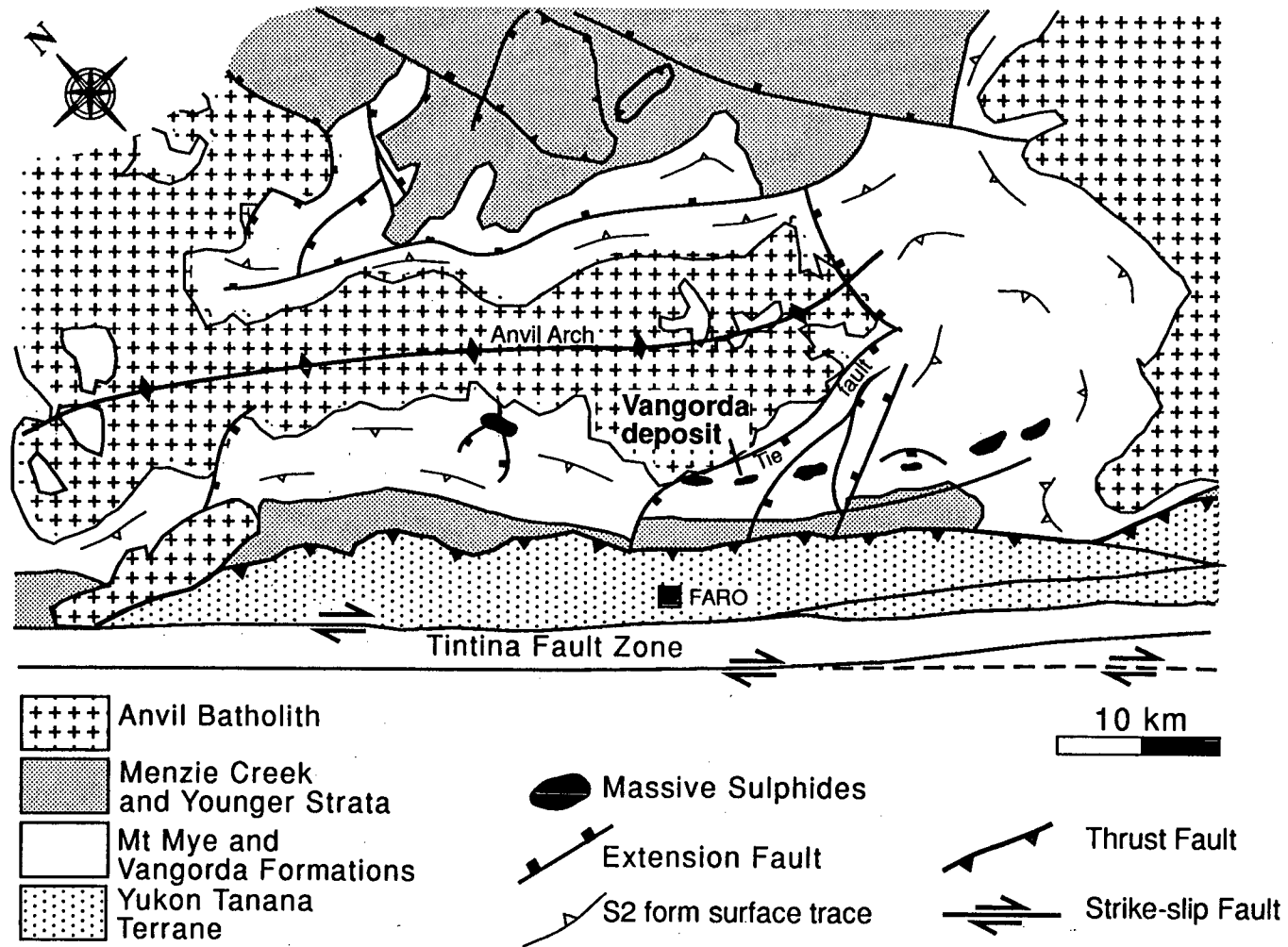
d)..Recrystallised pyrite showing preferred shape orientation. Plane polarised light, section 90-39, DDH 90V-67.

e). Pressure solution texture showing truncated grain boundaries and a preferred shape orientation. Nomarski interference contrast, section 90-41, DDH 90V-67.

f)..Annealed grains showing lobate grain boundaries and  $120^\circ$  triple junctions. Nomarski interference contrast, section 90-46, DDH 90V-116.

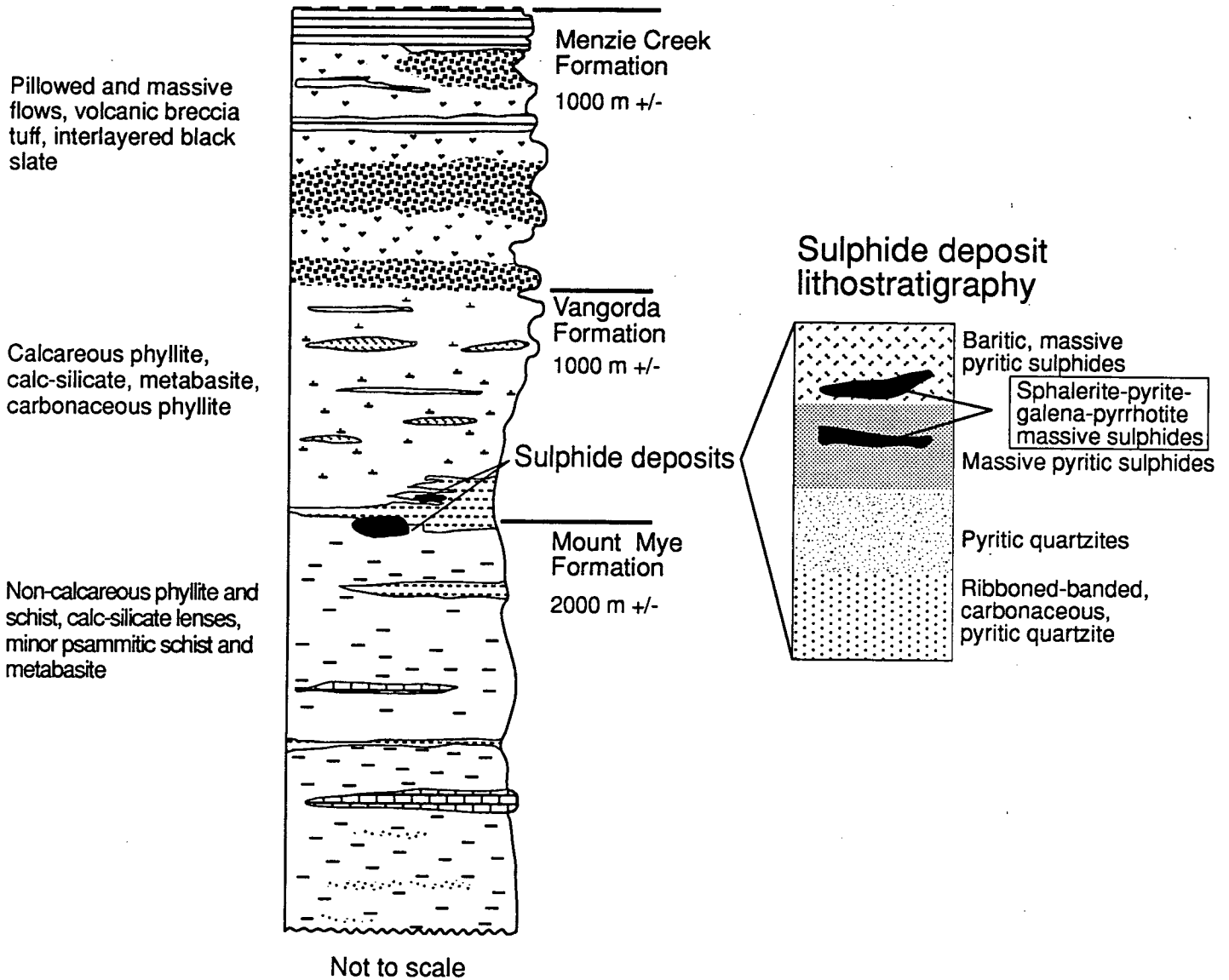


Brown 4 1/2 Clay 10/13



Brown & McClay Fig 2

# Anvil District Lithostratigraphy

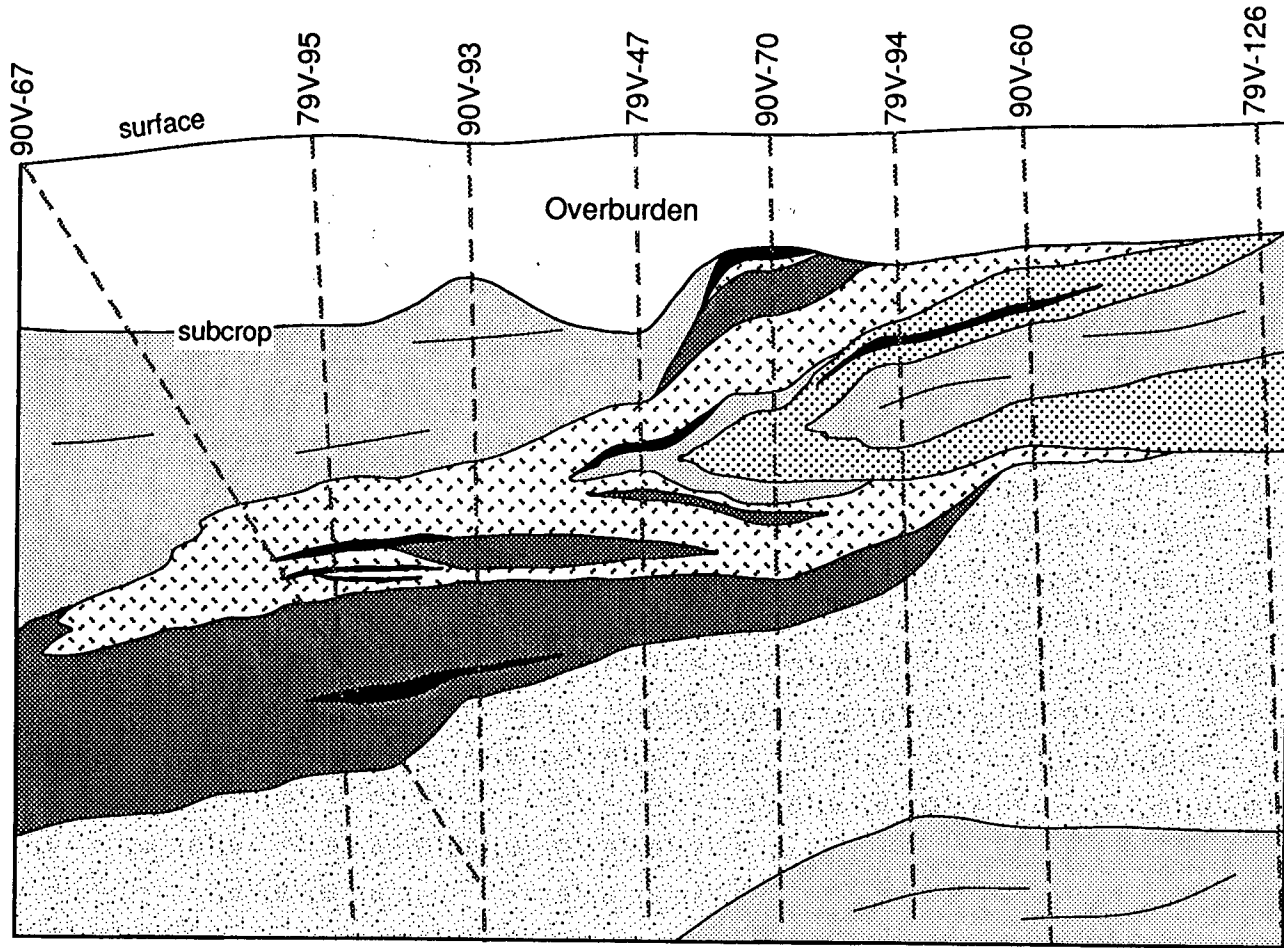


Brown & McCloy Fig. 3

SW

# Vangorda Deposit Section 6 E

NE



chlorite-muscovite phyllite

massive pyritic sulphide

ribbon-banded quartzite

pyritic quartzite

baritic massive sulphide

pyrrhotite-sphalerite-magnetite breccia

0 m V = H 50 m

Diamond  
drill hole

Brown & McClay fig. 4

79V-95

79V-47

79V-94

Well foliated phyllite with thin bands of baritic massive sulphide.

Tightly folded and boudinaged S1 py bands. M-asymmetry. Anastomosing pyrr + sph + mag shear zones containing tailed and rolled massive py breccia clasts.

Massive py with folded stringers (S1) of qtz and mag.

Folded S1 py banding. Locally developed, carbonaceous S2 foliation. Py porphyroblasts overgrow S2. Coarse-grained py, sph, mag and ga appear near lower contact.

Overburden

Contact not observed.

Brecciated contact

Sharp contact

Sharp contact

Sheared contact

Gradational contact

Cm to m-scale banded massive py. Variable pyrr and mag content. Pyrr coronas on py.

Penetrative S2 foliation. Coarse (up to 2mm) patches of pyrr.

Lithon textured.

Tightly folded py bands. Disseminated 0.2mm to 1.5mm py porphyroblasts. Pyrr and mag are common. Pyrr coronas on py. Weak S2.

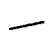
Isolated, intrafolial fold hinges with a chl S2 foliation. Py porphyroblasts aligned along S2.

## Legend

 fold asymmetry

 lithon texture

 fold closure

 S1, S2 trace

chl = chlorite

ga = galena

py = pyrite

pyrr = pyrrhotite

mag = magnetite

qtz = quartz

sph = sphalerite



Ribbon-banded, carbonaceous quartzite



Pyritic quartzite

Pyrrhotite + sphalerite + magnetite breccia



Massive pyritic quartzite



Baritic massive sulphide



Chlorite/muscovite phyllite

